Energy Loss and Charge Transfer of Argon in a Laser-Generated Carbon Plasma

A. Frank,[1] A. Blažević,[2] V. Bagnoud,[2] M. M. Basko,[3] M. Börner,[1] W. Cayzac,[1] D. Kraus,[1] T. Heßling,[2]
D. H. H. Hoffmann,[1] A. Ortner,[1] A. Otten,[1] A. Pelka,[1] D. Pepler,[4] D. Schumacher,[1] An. Tauschwitz,[5] and M. Roth[1]

[1]*Institut für Kernphysik, TU Darmstadt, Schlossgartenstraße 9, Darmstadt D-64289, Germany*
[2]*GSI Helmholtzzentrum für Schwerionenforschung GmbH, Planckstraße 1, Darmstadt D-64291, Germany*
[3]*ITEP, B. Cheremushkinskaja 25, Moscow 117259, Russia*
[4]*STFC Rutherford Appleton Laboratory, Harwell Oxford OX11 0QX, United Kingdom*
[5]*Institut für Theoretische Physik, Universität Frankfurt, Max-von-Laue-Strasse 1, Frankfurt 60438, Germany*
(Received 29 August 2012; published 12 March 2013)

This Letter reports on the measurement of the energy loss and the projectile charge states of argon ions at an energy of 4 MeV/u penetrating a fully ionized carbon plasma. The plasma of $n_e \approx 10^{20}$ cm^{-3} and $T_e \approx 180$ eV is created by two laser beams at $\lambda_{\mathrm{Las}} = 532$ nm incident from opposite sides on a thin carbon foil. The resulting plasma is spatially homogenous and allows us to record precise experimental data. The data show an increase of a factor of 2 in the stopping power which is in very good agreement with a specifically developed Monte Carlo code, that allows the calculation of the heavy ion beam's charge state distribution and its energy loss in the plasma.

The stopping of heavy ions in matter is a field of research that has been of great interest for more than a century. The first contributions to this field by Bohr [1], Bethe [2], and Bloch [3] are well known and have been further developed into much more advanced treatments [4–6]. The description of the interaction of heavy ion beams with cold matter has continuously evolved over the years and a good level of understanding has been reached, which is manifested in a relatively good agreement between theoretical predictions and experimental data [7]. However, the interaction with the fourth and actually most common state of matter in our Universe, the plasma, is only poorly understood and there is only very scarce reliable experimental data to test existing theories. The understanding of this subject, however, is most crucial to a variety of fields in modern physics, stretching from the realization of ICF (inertial confinement fusion) [8] and especially ion driven fast ignition [9,10], over astrophysics to the target response in modern accelerators like the LHC or the FAIR project. In the past, several experiments covering the field of low density plasmas ($n_e = 3 \times 10^{17}$ cm^{-3}) with an intermediate temperature of 2–3 eV produced by a gas discharge [11,12] have been conducted. In addition, the warm dense matter regime has been accessed via heavy ion beam heating [13] and shock waves [14]. The first stopping power experiments in laser-generated plasma have been conducted with temperatures up to 60 eV [15] and later for temperatures up to 250 eV [16]. In these experiments the plasma was directly created by a laser incident on a thin foil. However, these experiments were to a large degree dominated by the plasma target's hydrodynamic response to the inhomogeneities in a 1 mm scale laser focus profile [17]. Therefore, this Letter reports on the experimental results of the energy loss of argon ions in laser-generated plasma

created within a modified experimental scheme. The influence of the target's inhomogeneities is heavily reduced and hence the experiment allows us to study the atomic physics processes responsible for differences of up to a factor of two in the stopping power between the plasma and the cold target. The physical question that will be addressed in more detail is the significance of the consideration of the projectile charge state in a plasma environment for the determination of the stopping power. In a plasma, the cross sections for ionization and recombination change and lead to different projectile charge states directly affecting, in principle, any stopping power theory. Furthermore, at the energy considered here, the energy transfer needs to be modeled in an impact-parameter dependent way, since close collisions together with projectile screening play an important role. The measured results can be explained in detail by a specially developed Monte Carlo code calculating the charge transfer and the energy loss of the heavy ion beam in the plasma target taking the mentioned effects into account.

The experimental setup is shown in Fig. 1. The main improvements to earlier experiments [15,16] are the use of frequency-doubled laser beams and the irradiation of a thin carbon foil of 0.5 μm thickness from both sides. A higher laser frequency causes laser energy to be absorbed at higher plasma densities and hence to be more efficiently converted into thermal radiation, which is the key factor in smoothing out the density and temperature nonuniformities. The double-sided foil irradiation additionally accelerates the process of plasma heating, which is dominated by relatively slowly propagating quasidiffusive thermal waves. As a result, the amplitude and the lifetime of the plasma nonuniformities, induced by spatial laser intensity variations, are strongly reduced as compared to Ref. [16].
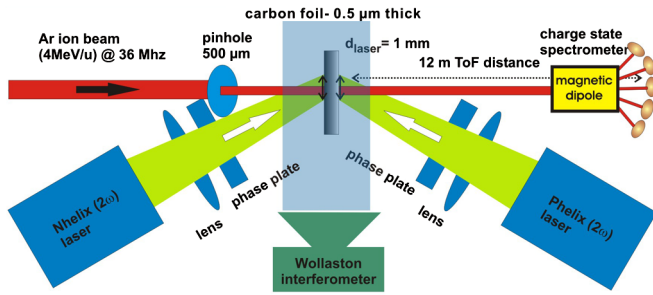
FIG. 1 (color online). Experimental setup for the energy loss and charge-transfer experiments.

FIG. 2 (color online). Temporal evolution of the Argon mean charge state after interacting with the plasma.

The laser pulses have been chosen to 30 J each at a pulse length of 7 ns (FWHM) which corresponds to an intensity of 4.6×10^{11} W/cm². This is sufficient to fully ionize the whole interaction volume at the end of the laser pulses. The laser focuses are created with the aid of random phase plates and have a diameter of 1 mm. In conclusion, after 6.5 ns a homogeneous plasma is created. The influence of the processes decreasing the quality of the previously recorded energy loss data is reduced by more than a factor of three (the details of the 2D hydrodynamic simulations are described in Ref. [17]). This allows us to analyze the details of the energy loss and projectile charge state distribution concerning the nature of the underlying atomic physics processes.

The plasma target is probed by an argon ion beam at an energy of 4 MeV/u at a pulse frequency of 36 MHz with pulse durations of 4 ns (FWHM). The diameter of the ion beam is reduced by a small pinhole to 500 μm. This assures that the ion beam only interacts with the central and most homogeneous part of the plasma of the same areal density. One goal of this setup is to distinguish between two different effects on the projectile's energy loss, the heavy ion's charge state and the differences in the Coulomb logarithm. The ions are then transported over 12 m distance onto a spectrometer [18] with 5 individual detectors based on polycrystalline diamond. Each records a separate charge state and hence covers more than 98% of the total projectile charge state distribution via selecting Ar^{14+} to Ar^{18+}. Since the different charge states of Argon have a different stopping power, these detectors not only serve as time of flight detectors but also to determine the charge state distribution of the ion beam after having interacted with the plasma.

For the determination of the projectile charge state distribution the recorded signals are integrated including the different responses of each detector to one single particle. The focus of this Letter is on the energy loss; hence, the most interesting parameter to judge the differences in the stopping power arising from the changing of the charge state distribution is the mean charge state of the projectile. In the experiment this parameter is determined after the interaction with the target. Its development in time
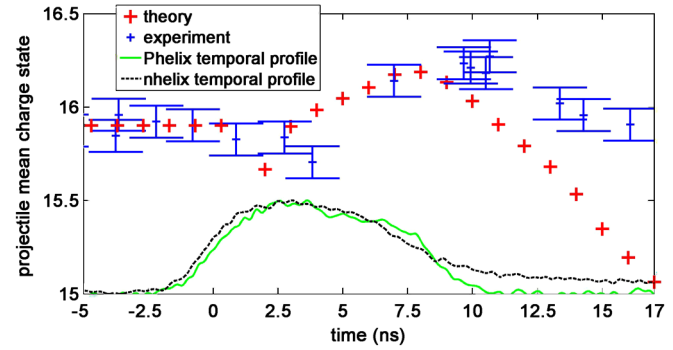
is shown in Fig. 2. For times earlier than 0 ns, which is the beginning of the laser irradiation on the target, the mean charge state after the interaction with the cold target foil is recorded. At 0 ns the two heating laser pulses start to irradiate the target. The jitter between the two laser pulses was 0.8 ns during the experimental campaign. The results shown are a superposition of 18 independent experiments with the same laser parameters with variations from shot to shot of less than 6% in energy. The temporal profiles of the lasers shown are exemplified from one laser shot. The spectrometer itself allows the recording of the number of incident particles with a precision of 6%–8% per charge state. For times earlier than 0 ns, a constant mean charge state of 15.8 for the solid target is measured which is in very good agreement with the expectations [19]. For the first 5 ns the differences between solid and the plasma state are within the error bars. However, for later times, between 7 and 12 ns, the mean charge state after the interaction with the plasma starts to exceed the one in cold matter. The maximum mean charge state measured is 16.2 and hence 0.4 charge states higher so the increase is not that significant. However, due to the nature of the plasma expansion, the target density decreases to $n_e = 10^{20}$ cm⁻³ after 7 to 12 ns. The stopping power of a gas compared to a solid-state body is lower [20], which is often called density effect. This effect can be judged by fitting formulas like Ref. [19] which gives $q_{mean,gas} = 15.1$. So in comparison to standard fitting formulas this already means an increase of the projectile mean charge state of $\Delta q_{mean} = 1.1$, which is significant, since this corresponds to a change in the stopping power of 10%.

A theoretical model to calculate the charge state distribution of the projectile has been proposed in Ref. [16]. This code uses experimentally determined cross sections for the charge transfer in cold matter [21]. The code is based on a modified version of ETACHA [22], which allows the calculation of the nonradiative and radiative electron capture as well as ionization and excitation during collisions with the target ions of the plasma. To take the density effect on the projectile charge state in the plasma into account, projectile shells are considered within a Monte Carlo approach

including excitation and decay, too. Since the plasma described in this Letter is fully ionized, the collisions with free electrons become more dominant. Hence, the model for dielectronic recombination previously used [16] has been improved by using Ref. [23]. However, for the microscopic description, the plasma parameters, electron, and ion density, temperature and ionization degree are needed both spatially and time resolved. Since this is not achievable with a sufficient accuracy from the plasma diagnostics in the experiment, we have to rely on hydrodynamic simulations with RALEF-2D [17]. The simulations, however, have been thoroughly benchmarked by our plasma diagnostics. Especially the time-resolved two-dimensional distributions of the electron density recorded with our multiframe Nomarski interferometer [24] have been used for this purpose and the hydrodynamic simulations show an excellent agreement with the experimental results, as shown in Fig. 3. The recorded electron densities from 3 separate laser shots recorded at the same time relative to the beginning of the heating lasers are plotted in comparison to the results of the simulations. Furthermore, this graph shows the reproducibility of the plasma formation with the setup using the second harmonic of the heating lasers [17].

The results for the mean charge states exiting the plasma in comparison with our model are also shown in Fig. 2. For times earlier than 11 ns the increase of the mean charge state is very well modeled. For later times the measured charge state exceeds the one predicted by the code. The maximum deviations between the stopping power calculated later in this Letter using the charge states obtained by the code and those obtained in the experiment is below 5% even at times around 15 ns. Since the calculation of charge-transfer cross sections is a complex many-particle problem, this method always inherently has certain errors and the agreement in this case is precise enough for the determination of the energy loss. The deviations due to the charge state are below the error bar of the energy loss data obtained in the experiment which is described in the following.

For the determination of the energy loss in the experiment the signals recorded by the spectrometer are numerically deconvoluted with the aid of the single particle responses. Then the center of mass of the deconvoluted signal is determined and used as arrival time for the time of flight measurements. Figure 4 shows the results for the energy loss. For the first two nanoseconds only very few deviations from the energy loss in the cold solid foil are detected. However, for later times a significant increase is recorded with a maximum energy loss of roughly 60% more than in the cold solid foil. The energy loss reaches its maximum after 8–10 ns when the whole plasma in the interaction region is fully ionized at the end of the laser pulse. For later times, the energy loss starts to decrease due to the 3D expansion of the plasma and reaches zero after 20 to 25 ns.

For a detailed and quantitative analysis of the effects contributing to the stopping power a theoretical approach is necessary. In the intermediate velocity regime charge transfer and hence projectile screening play an important role since the stopping power of any theory depends on the actual charge state of the ion in the target. Effective charge descriptions in the often used way of Northcliffe [25] have been shown to be unphysical and may lead to wrong results [26]. Instead, the Monte Carlo code mentioned above connects the actual charge state with the charge-dependent stopping powers calculated with the CASP code [27], which has been modified to describe the plasma case [16]. The CASP code interpolates between different impact-parameter regimes and hence also takes close and binary collisions into account which avoids, for example, the overestimation of the stopping power by the Bethe formula, which has been often used in the past also for the plasma case. The comparison for the energy loss presented in Fig. 4 shows a very good agreement. Three theoretical curves stemming from different simulations are shown in this picture. In the first one (red crosses), a completely homogenous focus profile for the hydrodynamic simulations has been assumed. Therefore, an immediate increase of the energy loss as soon as the laser starts irradiating the target is calculated. This is not found in the experimental data.
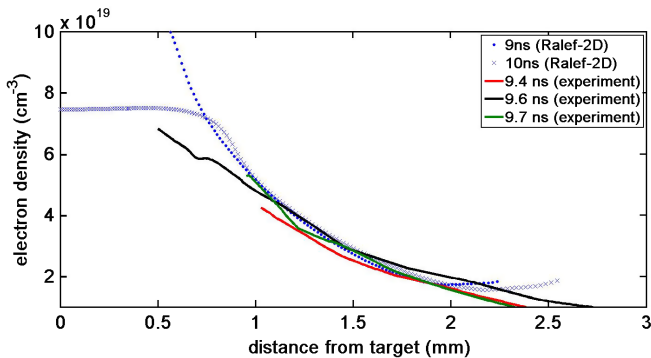

FIG. 3 (color online). Comparison between the recorded electron densities from 3 separate laser experiments and the results of RALEF-2D simulations.
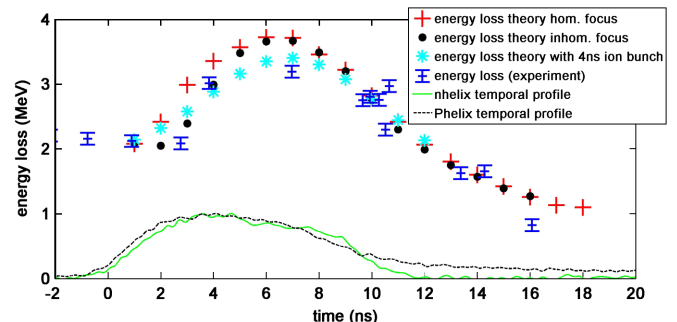

FIG. 4 (color online). Energy loss of argon at 4 MeV/u in the carbon plasma.

However, in this experimental scheme the laser focus profile is still not homogeneous, only the influence of the inhomogeneities is reduced. The second curve (black dots) includes the effects produced by a laser focus profile which has been simplified by a cosine-function $I(x) = I_0[1 + 0.5\cos(\omega x)]$ with a characteristic wavelength obtained from the focus profiles in the experiment of $\lambda = 50$ μm. The characteristic variation in the amplitude is 3 to 1 peak to valley. This does not represent the real laser profile of the random phase plates, this is impossible in a 2D simulation due to the nature of the random intensity distribution. Instead, it provides a quantitative estimate for the effects on the stopping power that are to be expected due to significantly reduced but still present plasma inhomogeneities (see Ref. [17]) at early times. Taking into account these effects improves the agreement between theory and experiment by delaying the rise of the stopping power with respect to the laser pulse. An additional improvement is achieved after we consider that the energy loss data are recorded with an ion beam of a pulse duration of 4 ns (FWHM). Because of the integration, the results already stop at 12 ns. The cyan curve shows the results which are obtained if the black curve is recorded with such a temporal Gaussian shape and the resulting agreement between theoretical values and experimental data becomes excellent.

The deviations between the experimental results and the theoretical predictions are below 10%. These results hence confirm the physical picture of the laser-induced plasma inhomogeneities as reported in earlier works [16,17] and the novel experimental setup has led to a substantial improvement of the experimental data and allows a detailed study of the underlying atomic physics: The contribution to the increase in the stopping power is dominated by the change in the coulomb logarithm, namely, the more efficient energy transfer to the plasmons. The change in the projectile mean charge state exiting the plasma from $q_{\mathrm{mean,solid}} = 15.8$ to $q_{\mathrm{mean,plasma}} = 16.2$ is not sufficient to explain the difference in the energy loss between the solid and the plasma phase. But considering the charge state distribution of the ion beam still remains important. First of all an actual value for the heavy ion charge state is needed and in addition the density of the target decreases over time. So for times between 7 and 12 ns at $n_e = 10^{20}$ cm^{-3} as shown in Fig. 3, the plasma more than compensates the gas-solid difference. This means according to the CASP models that around 85% of the stopping power increase in the target is due to the Coulomb logarithm, namely, the more efficient energy transfer to the plasmons, while 15% are due to the increase of the projectile charge states. This ratio however changes depending on projectile nuclear charge and energy. In total, an increase of a factor of 2 in the total stopping power is needed and calculated by our models to explain the difference found in the experimental data, because both the averaging over time and the slowly decreasing integral mass visible for the ion beam in the experiment due to the three dimensional plasma expansion decrease the energy loss values found in the experiment. This is in a very good agreement with the predictions of our combined theoretical model [16].

In summary, this Letter presents new experimental data for both the projectile charge states after penetrating a hot fully ionized carbon plasma and the energy loss of this ion beam. The temporal evolution of both parameters can be very well explained both qualitatively and quantitatively by our Monte Carlo code describing all relevant charge-transfer processes and the energy loss without the use of an effective charge description but including all relevant atomic physics processes. The stopping power is mainly increased due to the more efficient transfer to plasmons than to bound electrons while the role of the measured and calculated actual projectile charge states remains an important parameter. The physical connection for plasma has been established in this Letter.

[1] N. Bohr, Philos. Mag. **25**, 10 (1913).
[2] H. Bethe, Ann. Phys. (Berlin) **397**, 325 (1930).
[3] F. Bloch, Ann. Phys. (Berlin) **408**, 285 (1933).
[4] P. Sigmund and A. Schinner, Eur. Phys. J. D **12**, 425 (2000).
[5] P. L. Grande and G. Schiwietz, Phys. Rev. A **58**, 3796 (1998).
[6] G. Maynard, G. Zwicknagel, C. Deutsch, and K. Katsonic, Phys. Rev. A **63**, 052903 (2001).
[7] H. Paul, www.exphys.uni-linz.ac.at/stopping (2013).
[8] J. Nuckolls, L. Wood, A. Thiessen, and G. Zimmerman, Nature (London) **239**, 139 (1972).
[9] M. Tabak, J. Hammer, M. E. Glinsky, W. L. Kruer, S. C. Wilks, J. Woodworth, E. M. Campbell, M. D. Perry, and R. J. Mason, Phys. Plasmas **1**, 1626 (1994).
[10] M. Roth et al., Phys. Rev. Lett. **86**, 436 (2001).
[11] K. Weyrich et al., Nucl. Instrum. Methods Phys. Res., Sect. A **278**, 52 (1989).
[12] D. Gardes et al., Radiat. Eff. Defects Solids **110**, 49 (1989).
[13] D. H. H. Hoffmann et al., Nucl. Instrum. Methods Phys. Res., Sect. B **161–163**, 9 (2000).
[14] K. Weyrich, H. Wahl, A. Golubev, A. Kantsyrev, M. Kulish, S. Dudin, D. H. H. Hoffmann, B. Sharkov, and V. Mintsev, Nucl. Instrum. Methods Phys. Res., Sect. A **577**, 366 (2007).
[15] M. Roth, C. Stöckl, W. Süß, O. Iwase, D. O Gericke, R. Bock, D. H. H. Hoffmann, M. Geissel, and W. Seelig, Europhys. Lett. **50**, 28 (2000).
[16] A. Frank et al., Phys. Rev. E **81**, 026401 (2010).
[17] A. Tauschwitz, M. Basko, A. Frank, V. Novikov, A. Grushin, A. Blazevic, M. Roth, and J. A. Maruhn, High Energy Density Phys. **9**, 158 (2013).
[18] W. Cayzac et al., Rev. Sci. Instrum. (to be published).

[19] G. Schiwietz and P. L. Grande, Nucl. Instrum. Methods Phys. Res., Sect. B **175–177,** 125 (2001).

[20] N. E. B. Cowern, C. J. Woods, and C. J. Sofield, Nucl. Instrum. Methods **216,** 287 (1983).

[21] A. Blazevic, B. Rethfeld, and D. Hoffmann, K. Dan. Vidensk. Selsk. Mat. Fys. Medd. **52,** 109 (2006).

[22] J. P. Rozet, C. Stéphan, and D. Vernhet, Nucl. Instrum. Methods Phys. Res., Sect. B **107,** 67 (1996).

[23] Th. Peter, R. Arnold, and J. Meyer-ter-Vehn, Phys. Rev. Lett. **57,** 1859 (1986).

[24] M. Boerner *et al.*, Rev. Sci. Instrum. **83,** 043501 (2012).

[25] L. C. Northcliffe, Annu. Rev. Nucl. Part. Sci. **13,** 67 (1963).

[26] P. Sigmund and A. Schinner, Nucl. Instrum. Methods Phys. Res., Sect. B **174,** 535 (2001).

[27] http://www.helmholtz-berlin.de/people/gregor-schiwietz/casp_en.html (2011).